Experiments on metastable states of three-dimensional trapped particle clusters

D. Block,[1] S. Käding,[2] A. Melzer,[2] A. Piel,[1] H. Baumgartner,[3] and M. Bonitz[3]
[1]*IEAP, Christian-Albrechts-Universität, D-24098 Kiel, Germany*
[2]*Institut für Physik, Ernst-Moritz-Arndt-Universität, D-17487 Greifswald, Germany*
[3]*ITAP, Christian-Albrechts-Universität, D-24098 Kiel, Germany*

(Received 1 February 2008; accepted 7 March 2008; published online 10 April 2008)

Small three-dimensional charged-dust clusters, so-called Yukawa balls, are analyzed with regard to their construction principle. For that purpose, in an experimental approach, different (metastable) configurations of clusters with fixed particle number ($N<100$) have been generated under identical plasma and trapping conditions. Metastable states are frequently observed. In combination with molecular dynamics simulations, it is shown that particle interaction with screening strongly affects the appearance probabilities of metastable configurations. Small clusters show different average density distributions with screened interaction compared to pure Coulomb, although having the same ground state configurations. © *2008 American Institute of Physics*. [DOI: 10.1063/1.2903549]

Three-dimensional (3D) clusters consisting of few particles are of particular interest in various fields of physics and chemistry as their structure and dynamics depend strongly on the number of particles. Cold noble gases form clusters with icosahedral shell structure.[1,2] Similar structures were observed in alkali-metal, noble-metal, or Si clusters.[2,3] In many systems an enhanced stability is found for highly symmetric configurations. These magic numbers are found to be similar even for trapped charged particle systems,[4–6] which implies that geometric constraints determine the structure of different types of clusters to a large extent. On the other hand, it is observed that the type of bonding influences the structure of these clusters.[2]

Ordered states of trapped charged particles are formed when the coupling parameter $\Gamma=Z^2e^2/4\pi\epsilon_0 bkT$ exceeds a critical value, i.e., $\Gamma_{\mathrm{crit}}\simeq 180$, for infinite systems. Here, Z is the charge number of the particles and b the interparticle spacing. For ion clusters, the structure is a set of nested spherical shells.[4,7] Recently, similar structures have been discovered for highly charged microparticles ($Z\simeq 2000$) trapped in a gas-discharge plasma.[8,9] These so-called Yukawa balls reach the regime of strong coupling already at large interparticle distances ($b\approx 0.5$ mm) and room temperature ($T=300$ K); i.e., $\Gamma\simeq 500$. Additionally, Yukawa balls are highly transparent objects and the particle dynamics is sufficiently slow to be observed by means of video microscopy.

In contrast to ion crystals, the particles in Yukawa balls interact by a screened Coulomb potential with a screening length λ_D. Investigations of the ground state configuration in experiments as well as molecular dynamics (MD) and Monte Carlo simulations[10] have shown that in large clusters $N>100$ the shielded interaction affects the structure of the cluster. While pure Coulomb systems have strictly homogeneous density,[4,5] increased occupation numbers of inner shells and depletion of outer shell were observed in shielded systems. This inhomogeneous density distribution of Yukawa balls is a consequence of the change from a global force equilibrium (due to the particular properties of the far-reaching pure Coulomb interaction) to a local balance (due to the dominance of nearest neighbors in screened interaction).[11] Although this result was obtained in a fluid model for large systems, the comparison with simulations showed that systems with only thousand particles are accurately described by this approximation if correlation effects are taken into account.[12]

For small systems ($N<100$) the fluid approximation fails. Simulations[10] indicate that the ground state configuration of small Yukawa clusters ($\kappa=b/\lambda_D<1.5$) does not deviate systematically from pure Coulomb systems. However, there is no obvious reason that the principle that short range interaction leads to overpopulation of inner shells should not apply in small systems.

This ambiguity can be resolved by investigating the ground and metastable states of small clusters. It is well known that for many particle numbers, metastable configurations exist with energies moderately higher than the ground state.[5] To access these different metastable states in our experiments, we have repeatedly produced clusters of fixed particle number. The obtained cluster configurations are analyzed in view of their structure and their probability of appearance. This allows us to reveal the role of screening with respect to the structural properties of small clusters. The experimental results are compared with MD simulations.

The experiments have been conducted in a capacitively coupled rf-discharge at 13.56 MHz in argon. Monodisperse plastic spheres of 3.46 μm diameter are confined horizontally by a cubic glass tube placed on the lower electrode. Vertically, gravity is compensated by the combined action of an upward thermophoretic force due to heating of the lower electrode and a weak electric field.[13] In this trap, Yukawa balls are produced. An improved stereoscopic camera setup is used that consists of three synchronized cameras with pairwise perpendicular orientation. The whole particle cloud is illuminated by an expanded circular laser beam (600 mW at 532 nm). With this setup, the 3D positions of all particles in

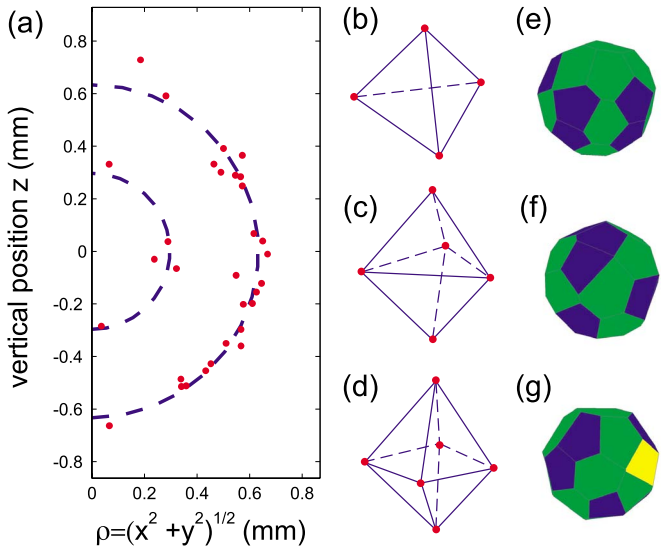

FIG. 1. (Color online) Structure of metastable configurations of the $N=31$ cluster. (a) Particle positions in cylindrical coordinates in the ρ-z plane. The red dots are the average particle positions of a (5,26) configuration. The dashed lines indicate the shell radii (R_i and R_o). (b)–(d) Average structure of the inner shell. The particle arrangement is shown for clusters with $N_i=4$ (b), $N_i=5$ (c), and $N_i=6$ (d) particles. (e)–(g) Voronoi analysis (blue (dark gray)–pentagons, green (medium gray)–hexagons, yellow (light gray)–defects) of the corresponding outer shell for $N_o=27$ (e), $N_o=26$ (f), and $N_o=25$ (g) particles. All plots show experimental results.

TABLE I. Results of the configuration repetition experiment with 37 realizations of a cluster with $N=31$ particles. $N_{i,o}$ denotes the number of particles, $R_{i,o}$ are the average shell radii of inner and outer shell, respectively. V_{WS} is the average Wigner–Seitz cell volume of a particle in the inner shell. For comparison, the results of a MD simulation at $\kappa=1.1$ with 500 runs of a 31-particle cluster are also shown. The simulation parameters are given in the text.

	Experiment		
	$N_i=4$	$N_i=5$	$N_i=6$
Abundance	13	23	1
Probability (%)	35 ± 10	62 ± 13	3 ± 3
R_i (mm)	0.262 ± 0.011	0.290 ± 0.006	0.322
R_o (mm)	0.632 ± 0.003	0.641 ± 0.003	0.643
$N_i/4\pi R_i^2$ (mm^{-2})	4.63 ± 0.37	4.74 ± 0.19	4.61
$N_o/4\pi R_o^2$ (mm^{-2})	5.37 ± 0.06	5.03 ± 0.06	4.81
V_{WS}(mm^3)	0.070 ± 0.002	0.068 ± 0.002	0.070
	Simulation		
Probability (%)	28 ± 4	63 ± 5	8 ± 2
R_i (mm)	0.250	0.280	0.303
R_o (mm)	0.631	0.639	0.647

a Yukawa ball can be measured simultaneously with high spatial and temporal resolution.[14]

In a first set of experiments, different metastable configurations of clusters with fixed total particle number were realized. Here, we restrict our discussion on clusters with about 30 particles because these particle numbers are well separated from magic configurations ($N=12$ and 57), where closed shell configurations are observed. Hence, due to partly filled shells these cluster promise to have several accessible metastable configurations.

To produce different metastable configurations, the following procedure was applied. After having trapped a cluster, a well adjusted variation of rf-power allows to interrupt the particle confinement for a few seconds, which destroys the Yukawa ball. However, before the particles leave the discharge, we re-established the trapping regime and the particles form a new stable cluster. This experimental procedure enabled us to fill the trap several times with the same particles, but without any memory of the previous configuration. The experiments have been performed in a single continuous run over about 2 h, in each loss-and-recovery cycle the cluster was allowed to relax for about a minute before the cluster realization has been recorded for 30 s.

The results of the repeated trapping experiment for a $N=31$ cluster are shown in Fig. 1 and Table I. A number of 37 realizations of the cluster have been generated at exactly the same plasma and confinement conditions (gas pressure $p=90$ Pa, discharge power $P=7.5$ W). All clusters are found to consist of two shells [Fig. 1(a)], but the shell population differs among these clusters. Clusters with $N_i=4$, 5, and 6 particles on the inner shell are observed. The particle arrangement on the inner shell is given in Figs. 1(b)–1(d). The observed structures are in perfect agreement with those expected from geometric considerations; namely, a tetrahedron for $N_i=4$, a double tetrahedron ($N_i=5$), and a bipyramid ($N_i=6$). As shown by the Voronoi cells in Figs. 1(e)–1(g), the particles on the outer shell arrange in an organized pattern of hexagons and pentagons as required for a hexagonal lattice bent onto a sphere. Hence, well defined crystalline clusters of different (metastable) states (4,27), (5,26), and (6,25) have been reliably produced in the experiment.

A more detailed picture is obtained when these clusters are analyzed quantitatively. First, the average shell radii for different realizations have only small standard deviations (see Table I), indicating that the different configurations are precisely reproduced in the experiment. Further, a significant increase in inner shell radius R_i with N_i is observed, whereas the outer shell radius R_o grows only weakly. However, the area density of the particles ($N_{i,o}/4\pi R_{i,o}^2$) is roughly constant for the inner shell, whereas it distinctly decreases with increasing N_i for the outer shell. Thus, the higher population on the inner shell goes along with a reduced charge density on the outer shell rather than with an increased cluster size. Second, the different configurations have different probability of realization. The configuration (5,26) occurred in about two thirds of the cases, (4,27) in about one third. The configuration (6,25) was seen only once. Note that the metastable configuration (5,26) appears more frequently than the ground state (4,27).

To clarify the experimental observations, we have performed MD simulations of the $N=31$ cluster. The crystalline state of the cluster at room temperature ($T=300$ K) requires a charge of $Z=2000$ in the simulation in agreement with previous investigations.[10,13] The curvature parameter $\alpha=5.20\times10^{-11}$ kg s^{-2} of the 3D isotropic parabolic trapping

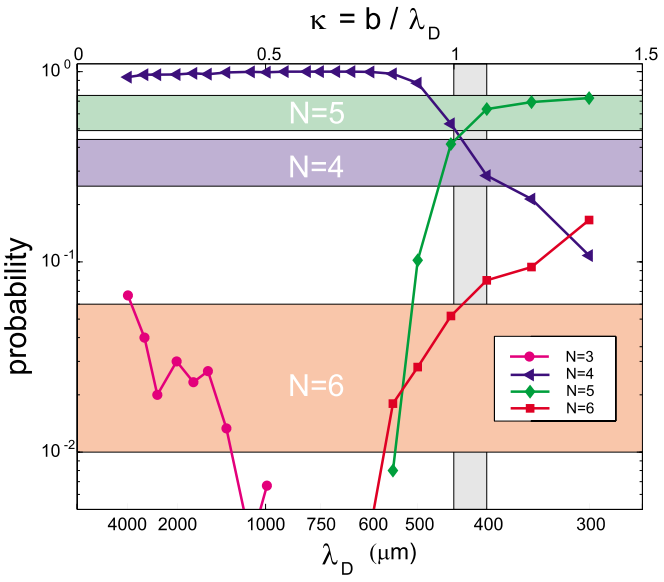

FIG. 2. (Color online) Probability of realization of configurations with N_i =3, 4, 5, and 6 particles on the inner shell for a N=31 cluster as a function of screening length λ_D. The experimental probabilities are indicated by the horizontal stripes. The matching value of κ is indicated by the vertical bar.

potential $V(r)=\frac{1}{2}\alpha r^2$ results from previous experiments[13] and from the observed particle density for N=31. Varying the screening length λ_D in the simulation, we can study the influence of short-range forces on the structure. The probability to find a certain metastable configuration in the simulation is shown in Fig. 2. The simulation is started from random particle positions to mimic the experimental loss and recovery of the confinement. The configuration (3,28), which has not been observed in the experiment, is found to have a nonvanishing probability only for $\lambda_D > 1000$ μm ($\kappa < 0.5$). In contrast, the experimentally observed configuration (6,25) only appears for $\lambda_D < 600$ μm ($\kappa > 0.78$). In this entire shielding range ($\kappa < 1.5$), the ground state configuration remains to be (4,27). Near λ_D=400 μm (κ=1.1), the simulated probabilities nicely arrive at the experimental ones (see Table I). This value of the screening length matches that determined from plasma simulations under similar conditions.[13] Even the shell radii of inner and outer shell of the simulated clusters at λ_D=400 μm have exactly the same absolute values for the different metastable configurations as the measurements (see Table I).

From numerous simulations with systematically varied parameters N, Z, T and α, we always find qualitatively the same distribution of appearance probabilities: The probability of metastable states with higher N_i increases with screening strength κ.

It is interesting to note that, as in the experiment, in the simulation the metastable state (5,26) is observed substantially more frequently than the ground state (4,27). The energy of the metastable configurations (5,26) and (6,25) is about 24 and 49 meV higher than the ground state, respectively. Thus, it is reasonable for dust clusters at room temperature that the metastable states are populated to a substantial degree. That the metastable state is found to be more probable than the ground state does not contradict statistical mechanics. A quantitative description of the appearance probabilities requires to consider the multiplicity of the different configurations as well as their vibrational and rotational degrees of freedom and is beyond the scope of this letter.

To generalize our findings, we performed additional experiments with different particle numbers and different plasma parameters. As a second example, a N=27 cluster is studied in a discharge with three times lower plasma power (p=70 Pa, P=2.5 W). The observed probabilities with 12 realizations of the N=27 cluster are $(46 \pm 14)\%$ for both the ground state (3,24) and metastable state (4,23), and $(8 \pm 6)\%$ for the metastable configuration (2,25). Correspondingly, the simulations show that the probabilities for (2,25) and (3,24) decrease with increasing screening strength, and that (2,25) is only observed for $\kappa < 0.80$. On the other hand, the probability for (4,23) increases with reduced screening length. Good agreement between experiment and simulation is found for κ=0.75; i.e., λ_D=750 μm. The increased Debye length λ_D for N=27 compared to the case of N=31 is a direct consequence of the reduced plasma density at reduced discharge power. These consistent findings validate our conclusions.

In a further experiment, we have investigated dynamical processes in such small clusters driven only by the kinetic temperature of the dust. The particle positions of a N=31 cluster were recorded for several minutes to search for self-excited transitions between metastable configurations. In the beginning of the sequence, the cluster remained for several minutes in a (4,27) configuration; only thermal motion of the particles about their equilibrium position was observed. At t=430 s a single particle starts to leave the outer shell at $r \approx 0.64$ mm, moves inwards, and reaches the innermost position (r=0.34 mm) at about t=517 s, where it resides for a short moment before it slowly returns to the outer shell. The radial trajectory of this particle is shown in Fig. 3(a). The radial positions of the other 30 particles stayed nearly constant. This transition is a very slow, gradual process. It is different from the hopping motion observed in 2D crystals occurring on the time scale of the Einstein frequency of nearest neighbor oscillations, which is of the order of a few hertz.[15]

Since we have the 3D particle positions at each time step, the variation of density profile and structure can be studied directly. The particle density is defined as the reciprocal volume of the Wigner–Seitz (WS) cell V_{WS} per particle. In our finite systems, the calculation of V_{WS} is possible only for the inner particles. Figure 3(b) shows the average WS volume per particle V_{WS} as the particle moves from the outer towards the inner shell.

The WS cell of the traveling particle can be computed when its radial position is $r < 0.55$ mm. Thus, for $r > 0.55$ mm, the cell volume V_{WS} is computed only for the four particles belonging to the inner shell. For $r < 0.55$ mm, the traveling particle is included in the computation of V_{WS}. It is seen that the V_{WS} in the configuration (4,27) is larger than that obtained when the traveling particle approaches the (5,26) configuration. For comparison, the average V_{WS} for the metastable configurations of the repetition experiment

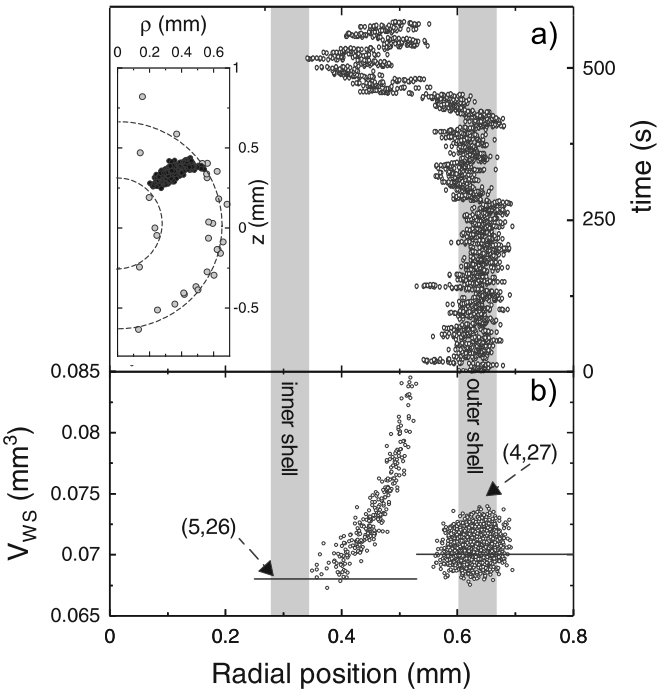

FIG. 3. (a) Radial component of the trajectory of the particle leaving the outer shell. The inset shows the particle trajectory in the ρ-z plane (black symbols). (b) Average Wigner–Seitz cell volume per particle for all particles belonging to the inner shell as a function of the radial position of the traveling particle. For $R<0.55$ mm, the Wigner–Seitz cell of the traveling particle is included in the average. The solid lines are the average V_{WS} of the configurations (4,27) and (5,26) obtained from the repetition experiment (see Table I).

(see Table I) are indicated by the horizontal solid lines.

When the traveling particle reaches the inner shell, a slight but significant decrease of V_{WS} is observed; i.e., the particle density on the inner shell increases for a (metastable) configuration with higher N_i. This demonstrates that indeed the density profile changes and that a higher population on the inner shell is not (completely) compensated by an increase in shell or cluster radius.

Therefore, our experiments show that the probability to observe a certain (metastable) configuration depends strongly on the interaction range: Configurations with larger N_i are preferred for smaller λ_D. Furthermore, the observed distribution of the configurations clearly implies a screened particle interaction with, on average, higher population of the inner shells and lower population on the outer.

Together with the result that configurations with larger N_i become more likely for increasing screening strength, these experiments show that, on average, even small Yukawa clusters have density profiles that are different from those of pure Coulomb systems. In effect, as for large clusters,[11,12] the inner shell is preferred at the expense of the outer. Hence, the dominance of short-range interaction has a measurable influence on the structure even for few-particle systems. Essentially, our results show that the probability of various configurations of small clusters is directly related to the interparticle interaction.

Metastable configurations of trapped particle systems can be reproducibly formed in the experiment, even far more often than the ground state. Besides their key role in understanding the structural properties of small clusters, they are of importance in melting processes, because transitions among metastable states mark the onset of melting. Since smaller systems melt at lower temperatures than larger systems,[16] small Yukawa balls promise to serve as ideal systems to gain insight into the microscopic processes of phase transitions in finite strongly coupled systems.

Financial support by the Deutsche Forschungsgemeinschaft via Grant Nos. SFB-TR24-A2, SFB-TR24-A3, SFB-TR24-A5, and SFB-TR24-A7 is gratefully acknowledged. We thank P. Ludwig for helpful discussions.

[1] A. L. Mackay, Acta Crystallogr. **15**, 916 (1962).
[2] F. Baletto and R. Ferrando, Rev. Mod. Phys. **77**, 371 (2005).
[3] O. Kostko, B. Huber, M. Moseler, and B. von Issendorff, Phys. Rev. Lett. **98**, 043401 (2007).
[4] R. W. Hasse and V. V. Avilov, Phys. Rev. A **44**, 4506 (1991).
[5] P. Ludwig, S. Kosse, and M. Bonitz, Phys. Rev. E **71**, 046403 (2005).
[6] D. H. E. Dubin and T. M. O'Neill, Rev. Mod. Phys. **71**, 87 (1999).
[7] A. Mortensen, E. Nielsen, T. Matthey, and M. Drewsen, Phys. Rev. Lett. **96**, 103001 (2006).
[8] O. Arp, D. Block, A. Piel, and A. Melzer, Phys. Rev. Lett. **93**, 165004 (2004).
[9] B. M. Annaratone, T. Antonova, D. D. Goldbeck, H. M. Thomas, and G. E. Morfill, Plasma Phys. Controlled Fusion **46**, 495 (2004).
[10] M. Bonitz, D. Block, O. Arp, V. Golubnychiy, H. Baumgartner, P. Ludwig, A. Piel, and V. Filinov, Phys. Rev. Lett. **96**, 075001 (2006).
[11] C. Henning, H. Baumgartner, A. Piel, P. Ludwig, V. Golubnichiy, M. Bonitz, and D. Block, Phys. Rev. E **74**, 056403 (2006).
[12] C. Henning, P. Ludwig, A. Filinov, A. Piel, and M. Bonitz, Phys. Rev. E **76**, 036404 (2007).
[13] O. Arp, D. Block, M. Klindworth, and A. Piel, Phys. Plasmas **12**, 122102 (2005).
[14] S. Kaeding and A. Melzer, Phys. Plasmas **13**, 090701 (2006).
[15] C.-L. Chan, W.-Y. Woon, and L. I, Phys. Rev. Lett. **93**, 220602 (2004).
[16] J. P. Schiffer, Phys. Rev. Lett. **88**, 205003 (2002).